Analytical Methods

Accepted Manuscript

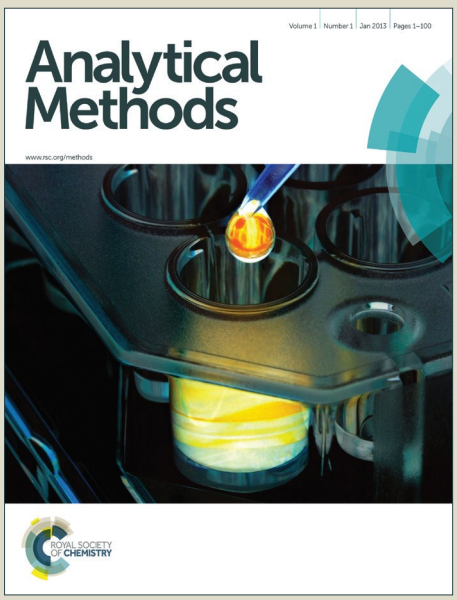

This is an *Accepted Manuscript*, which has been through the Royal Society of Chemistry peer review process and has been accepted for publication.

Accepted Manuscripts are published online shortly after acceptance, before technical editing, formatting and proof reading. Using this free service, authors can make their results available to the community, in citable form, before we publish the edited article. We will replace this *Accepted Manuscript* with the edited and formatted *Advance Article* as soon as it is available.

You can find more information about *Accepted Manuscripts* in the Information for Authors.

Please note that technical editing may introduce minor changes to the text and/or graphics, which may alter content. The journal's standard Terms & Conditions and the Ethical guidelines still apply. In no event shall the Royal Society of Chemistry be held responsible for any errors or omissions in this *Accepted Manuscript* or any consequences arising from the use of any information it contains.

ROYAL SOCIETY OF CHEMISTRY

www.rsc.org/methods

Acetylcholinesterase inhibition biosensor based on reduced graphene oxide/silver nanoclusters/chitosan nanocomposite for detection of organophosphorus pesticide

Yanli Zhang,[a] Hongjun Liu,[a] Zhongming Yang,[a] Shunlin Ji,[a] Junfang Wang,[a] Pengfei Pang,*[a] Lili Feng,[a] Hongbin Wang,[a] Zhan Wu[b] and Wenrong Yang[ac]

[a] Key Laboratory of Chemistry in Ethnic Medicinal Resources, Yunnan Minzu University, Kunming 650031, PR China

E-mail: pengfeipang@yahoo.com; fax: +86 871 65910017; tel: +86 871 65910017

[b] State Key Laboratory of Chemo/Biosensing and Chemometrics, Hunan University, Changsha 410082, PR China

[c] School of Life and Environmental Sciences, Deakin University, Geelong, VIC 3217, Australia

ABSTRACT

A sensitive electrochemical acetylcholinesterase (AChE) biosensor based on reduced graphene oxide (rGO) and silver nanoclusters (AgNCs) modified glassy carbon electrode (GCE) was developed. The rGO and AgNCs nanomaterials with excellent conductivity, catalysis and biocompatibility offered an extremely hydrophilic surface, which facilitated the immobilization of AChE to fabricate the organophosphorus pesticide biosensor. Carboxylic chitosan (CChit) was used as cross-linker to immobilize the AChE on rGO and AgNCs modified GCE. The AChE biosensor showed favorable affinity to acetylthiocholine chloride (ATCl) and could catalyze the hydrolysis of ATCl. Based on the inhibition of organophosphorus pesticide on the AChE activity, using phoxim as a model compound, the inhibition of phoxim was proportional to its concentration ranging from 0.2 to 250 nM with a detection limit of 81 pM estimated at a signal-to-noise ratio of 3. The developed biosensor exhibited good sensitivity, stability and reproducibility, thus providing a promising tool for analysis of enzyme inhibitors and direct analysis of practical samples.

1. Introduction

Organophosphorus pesticides (OPs) are widely employed in the field of agriculture owing to their high efficiency. Unfortunately, pesticide residues threat human health due to their high toxicity to acetylcholinesterase (AChE), which is essential for the function of central nervous system in humans.[1,2] Therefore, for human health safety and environmental protection purpose, it is very important to develop a sensitive, rapid, reliable and economical analytical method for detection and determination of these toxic substances. Comparison with the conventional analytical methods, such as liquid chromatography,[3,4] gas chromatography,[5,6] surface plasmon resonance,[7,8] and immunoanalytical techniques,[9] electrochemical biosensors with advantages of fast response, high sensitivity, low cost, miniaturization, and on-site analysis, have been a promising alternative to rapidly detect pesticides. Among them, AChE based electrochemical biosensors are particularly attractive due to their fast response and high sensitivity.[10] The principle of biosensors using AChE as a biological recognition element is based on the inhibition of the enzyme's natural catalytic activity by the agent that is to be detected.[11] The AChE immobilized on an electrode surface can catalyze the hydrolysis of acetylthiocholine chloride (ATCl) to produce an electro-active product of thiocholine (TCh), which used as a marker for pesticide detection. And the sustained prevalence of pollution continues to motivate the development of new biosensors for the detection of OPs in environmental and biological samples.

Nanostructured materials are excellent carriers due to their unique chemical and physical properties. Graphene-based hybrids with metals, metal oxides and polymers have received increasing attention during recent years, due to these hybrids affording significant physicochemical properties by effective adjustment or interaction of graphene sheets and incorporated materials.[12] A graphene-based nanocomposite has been developed as an enhanced sensing platform for biosensors because these kinds of nanocomposite films may generate synergistic effects to enhance the sensitivity.[13,14] Silver nanoclusters (AgNCs) have been widely used for developing of electrochemical sensing platforms due to its high conductivity, large surface area, excellent catalytic activity, and biocompatibility.[15–17] AgNCs exhibit high catalytic activity and could provide a suitable microenvironment to retain biological activity for biomolecule immobilization. AgNCs facilitate more efficient electron

transfer between the immobilized biomolecules and electrode substrates. This has led to the construction of electrochemical biosensors with enhanced analytical performance using AgNCs and graphene nanocomposite.[18,19]

Chitosin (Chit) is an abundant natural biopolymer with excellent film forming ability, biocompatibility and nontoxicity, which provides natural microenvironment to the enzyme and also gives sufficient accessibility to electrons to shuttle between the enzyme and the electrode.[20] Carboxylic chitosan (CChit) offers carboxyl to cross-linking with AChE and the covalent immobilization of enzyme, which results in greater stability and better biomolecule activity.[21–23]

In this work, rGO and AgNCs were synthesized by a chemical reduction method and characterized by transmission electron microscopy (TEM) and UV–vis absorption spectroscopy (UV–vis). The synthesized rGO and AgNCs with excellent conductivity, catalysis, and biocompatibility offered a hydrophilic surface for AChE adhesion. Furthermore, the specific affinity between the Ag and mercapto groups makes the thiocholine easily concentrate on the electrode surface, thus increasing the detection response. CChit was used as cross-linker to immobilize the AChE on rGO and AgNCs nanocomposte modified GCE. Finally, Chit was used as a protective membrane of the AChE biosensors to improve the stability of the biosensor. The biosensor exhibited excellent affinity to its substrate and the catalytic effect on the hydrolysis of ATCl. The biosensor has been demonstrated as a device with acceptable stability and reproducibility for the analysis of pesticides.

2. Experimental

2.1 Reagents and apparatus

Natural graphite powder, silver nitrate, carboxylic chitosan and sodium citrate were purchased from Sinopharm Chemical Reagent Co. Ltd. (China). Acetylcholinesterase (EC 3.1.1.7, 518 U mg^{-1} from electric eel), acetylthiocholine chloride, phoxim, *N*-(3-dimethylaminopropyl)- *N*′-ethylcarbodiimide (EDC) and *N*-hydroxysuccinimide (NHS) were purchased from Sigma-Aldrich (USA). Hydrazine solution was obtained from Fuchen Chemical Reagent Factory (Tianjin, China). All other chemicals and reagents were of analytical grade, and used as received. Phosphate buffer solution (PBS 20 mM) with different

pH values was used as supporting electrolytes. Deionized water was used through all experiments.

The electrochemical measurements were performed on a CHI660D electrochemical workstation (Shanghai, China). A standard three electrode cell was used for all electrochemical experiments with bare and modified glassy carbon electrode (GCE, d = 3 mm) as working electrode, a platinum (Pt) wire as an auxiliary electrode and an Ag/AgCl as a reference electrode, respectively. All experiments were performed at room temperature. UV–vis spectra were obtained on Agilent 8453 spectrophotometer. High-resolution transmission electron microscopy (HRTEM) was performed on a JEOL JEM-2100 Electron Microscope at an acceleration voltage of 200 kV.

2.2 Preparation of AgNCs

AgNCs were prepared according to a modified Lee and Meisel method.[24,25] All glassware was rigorously cleaned before use by treatment with aqua regia (HCl:HNO_3 = 3:1) followed by thorough rinsing with deionized water. A sample of $AgNO_3$ (25 mg) was dissolved in deionized water (250 mL) and heated rapidly to boiling under stirring. A solution of 1% trisodium citrate (5 mL) was added. The solution was kept on boiling gently for 20 min. The obtained AgNCs colloid solution was olive green. The concentration of synthesized AgNCs was ~30 μM, which as used directly for the fabrication of biosensors.

2.3 Synthesis of reduced graphene oxide

Graphene oxide (GO) was synthesized from natural graphite powder using a modified Hummers′ method.[26–29] Reduced graphene oxide (rGO) was prepared by the chemical reduction of GO using hydrazine as the reducing agent. Briefly, the GO (150 mg) was dispersed in deionized water (100 mL) by ultrasonication for more than 2 h. After that, hydrazine solution (3 mL) was added to the above homogeneous dispersion. The resulting solution was then refluxed at 95 °C for 24 h. The filter cake was washed with water and methyl alcohol for several times and finally dried at 60 °C.

2.4 Fabrication of AChE@CChit/AgNCs/rGO/GCE biosensor

Prior to modification, the glassy carbon electrode (GCE, 3 mm in diameter) was polished with 0.3 μm and 0.05 μm alumina slurry, and then ultrasonically cleaned in water, ethanol and water for 2 min, respectively. The electrode was allowed to dry in a stream of nitrogen. The modified electrodes were prepared by a simple casting method. Typically, an aliquot of 10 μL rGO aqueous dispersion (1 mg mL^{-1}) was dropped on the surface of the electrode and dried in air. Then, 10 μL of the AgNCs solution was coated on the rGO/GCE and dried at room temperature. Afterwards, 6 μL of AChE@CChit aqueous solution (0.04 U μL^{-1} AChE, 0.15% CChit, 1 mM NHS and 1 mM EDC, 20 mM PBS) was dropped onto the AgNCs/rGO/GCE and then dried overnight at 4 °C. Finally, the modified electrode (AChE@CChit/AgNCs/rGO/GCE) was rinsed with 20 mM PBS and covered with 3 μL 0.1% (wt %) chitosan solution as a protective membrane and then stored at 4 °C. As a control, AChE@CChit/rGO/GCE and AChE@CChit/AgNCs/GCE were also produced. The fabricating processes of the AChE biosensor are shown in Scheme 1.

2.5 Electrochemical measurements

The obtained biosensor was immersed in PBS solutions containing different concentrations of phoxim for 10 min, and then transferred to an electrochemical cell of 10 mL PBS (pH 7.0) containing 1.0 mM ATCl to test the electrochemical response. The inhibition rate of phoxim was calculated as follows:

$$\text{Inhibition (\%)} = (I_{p,control} - I_{p,exp})/I_{p,control} \times 100\%$$

where $I_{p,control}$ and $I_{p,exp}$ were the peak currents of ATCl on AChE@CChit/rGO/GCE without and with organophosphorus pesticide inhibition, respectively. Inhibition (%) was plotted against the concentration of the pesticide to obtain linear calibration curve.

3. Result and discussion

3.1 Characterization of rGO and AgNCs

The morphologies of the as-prepared rGO and AgNCs were investigated by employing HRTEM. As shown in Fig. 1A, it was observed that a few layers of crumpled sheets of rGO morphology with a wrinkled paper-like structure, which is beneficial for maintaining a high surface area and dispersion of nanopaticles on the surface of the electrode. Fig. 1B showed

the TEM of synthesized AgNCs. The AgNCs with a diameter of ~2 nm, were distributed uniformly, which minimized the barrier of the electron transfer between rGO layers and resulted in the excellent electrochemical property. We investigated the as-prepared AgNCs by UV-vis spectroscopy. As shown in Fig. 2, narrow absorption peak at 400 nm was observed, indicating the monodispersion of spherical AgNCs, which is consistent with the previous report.[25] These characterizations proved the successful preparation of rGO and AgNCs.

3.2 Electrochemical behavior of AChE@CChit/AgNCs/rGO/GCE

Cyclic voltammetry (CV) was employed to evaluate the performance of the fabricated biosensor during stepwise modification. Fig. 3A shows the cyclic voltammetric curves of different AChE modified electrodes in the presence of 1.0 mM ATCl in pH 7.0 PBS. As shown in Fig. 3A, AChE can hydrolyze ATCl to produce thiocholine, which shows an irreversible oxidation peak at 0.74 V (curve c). No amperometric response could be observed at AChE@CChit/AgNCs/GCE (curve a) and AChE@CChit/rGO/GCE (curve b). The improvement of the oxidation signal for the AChE biosensor results from the excellent conductivity of the rGO sheets and the well biocompatibility and electrocatalytic property of the AgNCs. AgNCs/rGO provided an extremely hydrophilic surface for AChE adhesion. The AgNCs/rGO possessed excellent conductivity, catalytic activity and biocompatibility which were attributed to the synergistic effects of AgNCs and rGO. CChit was used to immobilize enzymes on the surface of AgNCs/rGO/GCE, keep the enzyme activities and improve electrons to shuttle between the enzyme and the electrode. Besides, Chit protective membrane was used to prevent the loss of the enzyme molecules, improve the anti-interference ability of the biosensor and provide a biocompatible microenvironment to maintain enzymatic activity. Furthermore, the specific affinity between the Ag and mercapto groups makes the thiocholine easily concentrate on the electrode surface, thus increasing the amperometric response.

Fig. 3B displays the typical cyclic voltammograms of AChE@CChit/AgNCs/rGO/GCE biosensor in the absence and presence of 1 mM ATCl in pH 7.0 PBS. No peak was observed at AChE@CChit/AgNCs/rGO/GCE (curve a) in 20 mM PBS. While 1.0 mM ATCl was added, an irreversible oxidation peak at 0.74 V was observed at AChE@CChit/AgNCs/rGO/GCE (curve b), attributed to the oxidation of thiocholine, the hydrolysis product of ATCl catalyzed

by immobilized AChE. The results demonstrate that AChE could retain its bioactivity when cross-linking with CChit and immobilized on AgNCs-rGO/GCE.

3.3 Optimization of experimental parameters

To improve the sensitivity of the AChE@CChit/AgNCs/rGO/GCE, the experimental parameters, such as buffer pH, enzyme loading amount, incubation time and ATCl concentration were optimized by CV. The bioactivity of the immobilized AChE depended on the buffer pH. Fig. 4A showed the relationship between catalytic amperometric response of AChE to ATCl and solution pH in 20 mM PBS containing 1.0 mM ATCl. The maximum peak current was obtained at about pH 7.0 in the pH range from 4.0 to 10.0. Thus, pH 7.0 was chosen in the following experiments.

Another important aspect for the preparation of biosensor was the loading amount of AChE. The effect of the loading amount on the biosensor ranging from 4 μL to 10 μL was investigated in 20 mM PBS (pH 7.0) containing 1.0 mM ATCl. As shown in Fig. 4B, the amperometric response increased with increasing amount of AChE and reached the maximum at about 6 μL, then decreased obviously when the amount of AChE was increased further. This phenomenon could be attributed to the higher resistance for the electrochemical processes which was caused by the increase of AChE film's thickness. Therefore, 6 μL AChE was selected as the optimal enzyme amount.

The inhibition time was one of the most influential parameters in the pesticide analysis. Therefore, the dependence of the phoxim on incubation time was also studied in a pesticide solution (5 nM). As shown in Fig. 4C, phoxim displayed an increasing inhibition to AChE with the increase of immersion time (2 to 14 min), and when the incubation time was longer than 10 min, the curve trended to a stable value, indicating that the binding interaction with active target groups in the enzyme reached saturation. However, the maximum value of inhibition was not 100%, which was likely attributed to the binding equilibrium between pesticides and binding sites in the enzyme. Thus, a 10 min incubation time was used in subsequent experiments.

The amperometric response of the biosensor to ATCl in 20 mM PBS was also investigated. As shown in Fig. 4D, with increasing ATCl concentration from 0.03 to 4.0 mM, the

amperometric response of the biosensor increases. The amperometric response of the biosensor was a linear function of ATCl concentration in two segments. With a further increase in ATCl concentration, a response plateau appeared, showing the characteristics of Michaelis–Menten kinetics.[30,31] The results indicate that the AChE@CChit/AgNCs/rGO/GCE biosensor had a great affinity and catalysis to its substrate ATCl. On the basis of these results, 1.0 mM ATCl was selected for further inhibition experiments and real sample detecting.

3.4 Inhibition measurements

Based on the inhibition of phoxim on the immobilized AChE activity, a simple and effective way for monitoring phoxim was successfully proposed. The inhibition effect of phoxim was investiaged by DPV measuring the amperometric response of biosensor to 1.0 mM ATCl after incubation for 10 min by different concentration of phoxim. The DPV was performed from 0.5 to 0.8 V with pulse amplitude of 50 mV, pulse width of 50 ms, and scan rate of 100 mV s^{-1}. As shown in Fig. 5A, with the response of the biosensor before and after 10 min of incubation in 2×10^{-10}, 4×10^{-10}, 6×10^{-10}, 1.5×10^{-9}, 4.5×10^{-9}, 1.5×10^{-8}, 6.0×10^{-8}, and 2.5×10^{-7} M phoxim, the peak currents (curves $b \rightarrow i$) dramatically decreased compared with that on the control (curve a), and the decrease in peak current increased with the increasing concentration of phoxim. Calibration plot of inhibition percentage *versus* phoxim concentration is shown in Fig. 5B. Linear equations of phoxim was $I(\%) = 23.806 \log c + 5.296$ from 0.2 nM to 250 nM with a correlation coefficient of 0.9966, and the detection limit was estimated to be 81 pM at a signal-to-noise ratio of 3. The analytical performance of the resulting biosensor is compared with other reported electrochemical sensors for detection of phoxim, including the enzyme-based and non-enzyme sensors, and the results are summarized in Table 1. It can be seen that the proposed biosensor exhibited a lower detection limit and a wider range. The higher sensitivity can be ascribed to the large surface area of rGO to increase the loading amount of AChE and the specific affinity between the Ag and mercapto groups to facilitate the thiocholine easily concentrate on the electrode surface, thus increasing the detection response. The results demonstrate that the proposed biosensor exhibits a satisfactory performance in terms of detecting trace amounts of pesticide phoxim.

3.5 Reproducibility and stability of biosensor

The reproducibility of the biosensors was evaluated by assaying five different electrodes in 1.0 mM ATCl after being immersed in 20 nM phoxim for 10 min. The relative standard deviation (RSD) was found to be 4.7%, indicating an acceptable reproducibility. Similarly, the intra-assay precision of the biosensor was estimated by assaying one enzyme electrode for five replicate measurements. RSD was found to be 3.8%, which proved a good repeatability. The long-term storage stability was a critical issue for practical application of the proposed biosensor. The prepared AChE@CChit/AgNCs/rGO/GCE biosensor was stored at 4 °C when not in use. No obvious decrease in the response of ATCl was observed in the first 7-day storage. After a 30 day storage period, the biosensor retained 92% of its initial current response, indicating a good storage stability.

3.6 Analysis of real samples

To investigate the practicality and reliability of an analytical method, spike recovery is a useful tool. A standard addition method was adopted to estimate the accuracy of the proposed biosensor. Table 2 shows the results obtained by analysis of these spiked samples. The recoveries of the tap water were observed in the range of 89.7 to 96.6%. The low relative standard deviations for phoxim demonstrated the high precision of analysis. The results indicated that the biosensor exhibited a good accuracy for the pesticides sensing in real samples and a great potential for practical application.

4. Conclusions

In summary, combining the advantageous characteristics of rGO and AgNCs, a novel AChE biosensor based on rGO–AgNCs has been developed. The AChE was selected as the model enzyme to evaluate the functionalization and the potential of rGO-AgNCs as versatile enzyme immobilization nanomaterials for the biosensor deign. The rGO-AgNCs nanocomposites showed excellent conductivity and biocompatibility, which had larger surface areas that were favorable for AChE adhesion and improve stability of the AChE biosensor. The constructed biosensor exhibited many merits such as high sensitivity, wide linear

response range, low detection limit, good fabrication reproducibility, and acceptable stability. Moreover, it can also be used for direct analysis of practical samples, which would be a new promising tool for pesticides analysis.

Acknowledgements

The authors gratefully acknowledge the financial support from the National Natural Science Foundation of China (21205104, and 21463028), International Education Cooperation Base of Yunnan Minzu University (YMU 218-02001001002129), Students' Experimental Practice Ability Enhancement Project of Yunnan Minzu University, Teaching Quality and Reform Project of Yunnan Province (2013027), and partially supported by the open funding project of the State Key Laboratory of Chemo/Biosensing and Chemometrics (2013014), Hunan University, PR China.

References

1 D. M. Quinn, *Chem. Rev.*, 1987, **87**, 955–979.

2 S. Andreescu and J. L. Marty, *Biomol. Eng.*, 2006, **23**, 1–15.

3 K. Buonasera, G. D'Orazio, S. Fanali, P. Dugo and L. Mondello, *J. Chromatogr. A*, 2009, **1216**, 3970–3976.

4 K. Seebunrueng, Y. Santaladchaiyakit and S. Srijaranai, *Talanta*, 2015, **132**, 769–774.

5 E. Ballesteros and M. J. Parrado, *J. Chromatogr. A*, 2004, **1029**, 267–273.

6 X. P. Liu, B. Mitrevski, D. K. Li, J. Q. Li and P. J. Marriott, *Microchem. J.*, 2013, **111**, 25–31.

7 T. J. Lin, K. T. Huang and C. Y. Liu, *Biosen. Bioelectron.*, 2006, **22**, 513–518.

8 E. Mauriz, A. Calle, J. J. Manclús, A. Montoya, A. M. Escuela, J. R. Sendra and L. M. Lechuga, *Sens. Actuators, B*, 2006, **118**, 399–407.

9 C. R. Suri, R. Boro, Y. Nangia, S. Gandhi, P. Sharma, N. Wangoo, K. Rajesh and G. S. Shekhawat, *Trends Anal. Chem.*, 2009, **28**, 29–39.

10 C. S. Pundir and N. Chauhan, *Anal. Biochem.*, 2012, **429**, 19–31.

11 H. Schulze, S. Vorlová, F. Villatte, T. T. Bachmann and R. D. Schmid, *Biosen. Bioelectron.*, 2003, **18**, 201–209.

12 M. S. Artiles, C. S. Rout and T. S. Fisher, *Adv. Drug Deliv. Rev.*, 2011, **63**, 1352–1360.

13 M. Pumera, A. Ambrosi, A. Bonanni, E. L. K. Chng and H. L. Poh, *Trends Anal. Chem.*, 2010, **29**, 954–965.

14 S. X. Wu, Q. Y. He, C. L. Tan, Y. D. Wang and H. Zhang, *Small*, 2013, **9**, 1160–1172.

15 M. Farrag, M. Thämer, M. Tschurl, T. Bürgi and U. Heiz, *J. Phys. Chem. C*, 2012, **116**, 8034–8043.

16 S. Huang, C. Pfeiffer, J. Hollmann, S. Friede, J. J. C. Chen, A. Beyer, B. Haas, K. Volz, W. Heimbrodt, J. M. M. Martos, W. Chang and W. J. Parak, *Langmuir*, 2012, **28**, 8915–8919.

17 C. C. Shen, X. D. Xia, S. Q. Hu, M. H. Yang and J. X. Wang, *Anal. Chem.*, 2015, **87**, 693–698.

18 X. X. Liu, X. W. Xu, H. Zhu and X. R. Yang, *Anal. Methods*, 2013, **5**, 2298–2304.

19 Y. J. Liu, G. C. Wang, C. P. Li, Q. Zhou, M. Wang and L. Yang, *Mater. Sci. Eng. C*, 2014, **35**, 253–258.

20 A. Sassolas, L. J. Blum and B. D. Leca-Bouvier, *Biotech. Adv.*, 2012, **30**, 489–511.

21 S. K. Shukla, A. K. Mishra, O. A. Arotiba and B. B. Mamba, *Int. J. Biol. Macromol.*, 2013, **59**, 46–58.

22 X. Wei, J. Cruz and W. Gorski, *Anal. Chem.*, 2002, **74**, 5039–5046.

23 T. Jeyapragasam and R. Saraswathi, *Sens. Actuators, B*, 2014, **191**, 681–687.

24 P. C. Lee and D. Meisel, *J. Phys. Chem.*, 1982, **86**, 3391–3395.

25 C. H. Munro, W. E. Smith, M. Garner, J. Clarkson and P. C. White, *Langmuir*, 1995, **11**, 3712–3720.

26 W. S. Hummers and R. E. Offeman, *J. Am. Chem. Soc.*, 1958, **80**, 1339.

27 S. Stankovich, D. A. Dikin, R. D. Piner, K. A. Kohlhaas, A. Kleinhammes, Y. Y. Jia, Y. Wu, S. T. Nguyen and R. S. Ruoff, *Carbon*, 2007, **45**, 1558–1565.

28 Y. L. Zhang, Y. P. Liu, J. M. He, P. F. Pang, Y. T. Gao and Q. F. Hu, *Electrochim. Acta*, 2013, **90**, 550–555.

29 Y. L. Zhang, S. X. Xiao, J. L. Xie, Z. M. Yang, P. F. Pang and Y. T. Gao, *Sens. Actuators, B*, 2014, **204**, 102–108.

30 Y. Y. Zheng, Z. M. Liu, Y. F. Jing, J. Li and H. J. Zhan, *Sens. Actuators, B*, 2015, **210**, 389–397.

31 Q. Liu, A. R. Fei, J. Huan, H. P. Mao and K. Wang, *J. Electroanal. Chem.*, 2015, **740**, 8–13.

32 X. X. Lu, H. P. Bai, Q. Ruan, M. H. Yang, G. M. Yang, L. Tan and Y. H. Yang, *Int. J. Environ. Anal. Chem.*, 2008, **88**, 813–824.

33 Y. H. Yang, M. M. Guo, M. H. Yang, Z. J. Wang, G. L. Shen and R. Q. Yu, *Int. J. Environ. Anal. Chem.*, 2005, **85**, 163–175.

34 H. S. Yin, S. Y. Ai, J. Xu, W. J. Shi and L. S. Zhu, *J. Electroanal. Chem.*, 2009, **637**, 21–27.

35 X. Sun and X. Y. Wang, *Biosen. Bioelectron.*, 2010, **25**, 2611–2614.

36 M. Y. Chao and M. F. Chen, *Food Anal. Method.*, 2014, **7**, 1729–1736.

37 C. Zhang, J. X. Zhang, K. Wang and Z. H. Dai, *Acta Chim. Sinica*, 2012, **70**, 1008–1012.

38 L. H. Wu, W. Lei, Z. Han, Y. H. Zhang, M. Z. Xia and Q. L. Hao, *Sens. Actuators, B*, 2015, **206**, 495–501.

39 Y. H. Zheng, A. W. Wang, H. T. Lin, L. Fu and W. Cai, *RSC Adv.*, 2015, **5**, 15425−15430.

Figure captions:

Scheme 1 Schematic illustration of the biosensor fabrication and the principle for OPs determination.

Fig. 1 HRTEM images of rGO (A) and AgNCs (B).

Fig. 2 UV-vis absorption spectrum of the as-synthesized AgNCs.

Fig. 3 (A) Cyclic voltammograms of AChE@CChit/AgNCs/GCE (a), AChE@CChit/rGO/GCE (b), and AChE@CChit/AgNCs/rGO/GCE (c) in 20 mM PBS (pH 7.0) containing 1.0 mM ATCl. (B) Cyclic voltammograms of AChE@CChit/AgNCs/rGO/GCE in the absence (a) and presence (b) 1.0 mM ATCl in 20 mM PBS (pH 7.0). Scan rate: 0.05 V s^{-1}.

Fig. 4 Effect of pH (A) and AChE amount (B) on the amperometric response of the AChE@CChit/AgNCs/rGO/GCE in 20 mM PBS containing 1.0 mM ATCl. (C) Effect of incubation time on the inhibition rate of the AChE@CChit/AgNCs/rGO/GCE in 20 mM PBS (pH 7.0) containing 1.0 mM ATCl and 2 nM phoxim. (D) Amperometric response of the AChE@CChit/AgNCs/rGO/GCE to different concentration of ATCl in 20 mM PBS (pH 7.0).

Fig. 5 (A) DPV of the AChE@CChit/AgNCs/rGO/GCE in 20 mM PBS containing 1.0 mM ATCl after incubation with ($a \rightarrow i$) 0, 2×10^{-10}, 4×10^{-10}, 6×10^{-10}, 1.5×10^{-9}, 4.5×10^{-9}, 1.5×10^{-8}, 6.0×10^{-8} and 2.5×10^{-7} M phoxim for 10 min. (B) Linear relationships between the inhibition percentage and phoxim concentration.

Table 1 Comparison of performance of the other electrochemical sensors for phoxim detection[a]

Table 2 Determined results of phoxim in spiked water samples (n = 5)

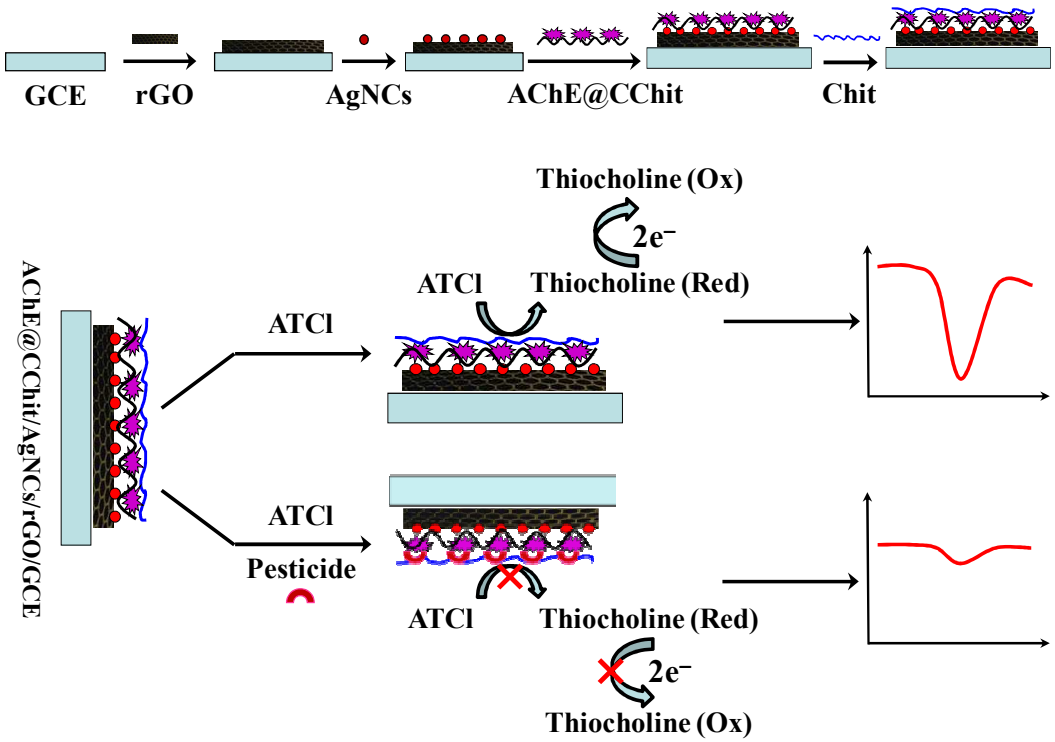

Scheme 1

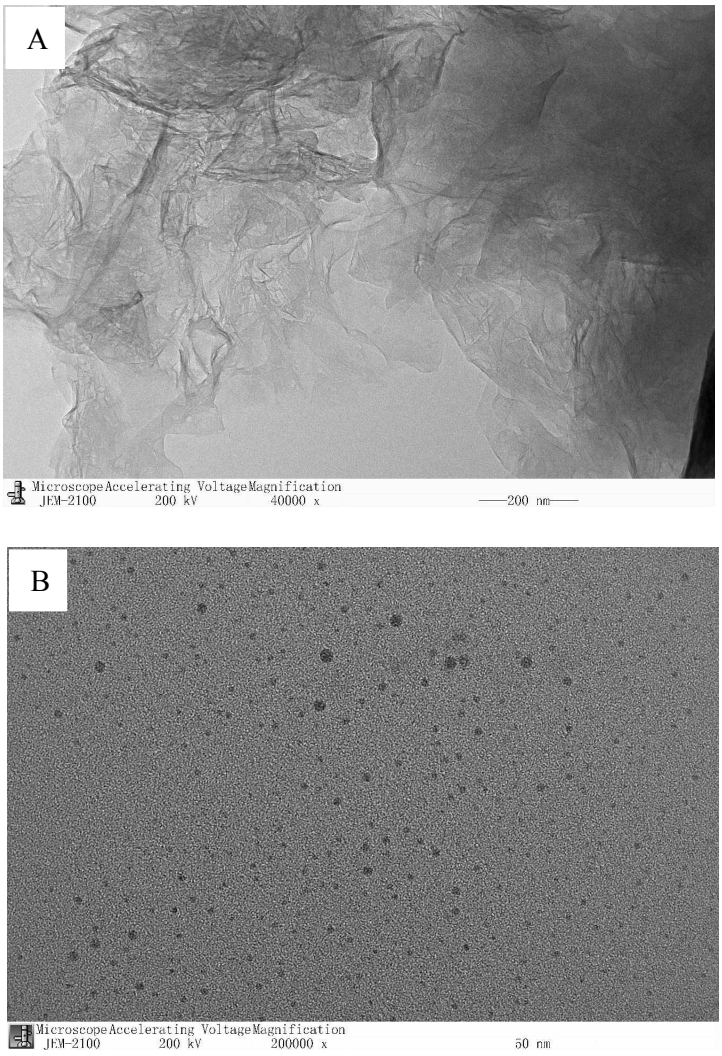

Fig. 1

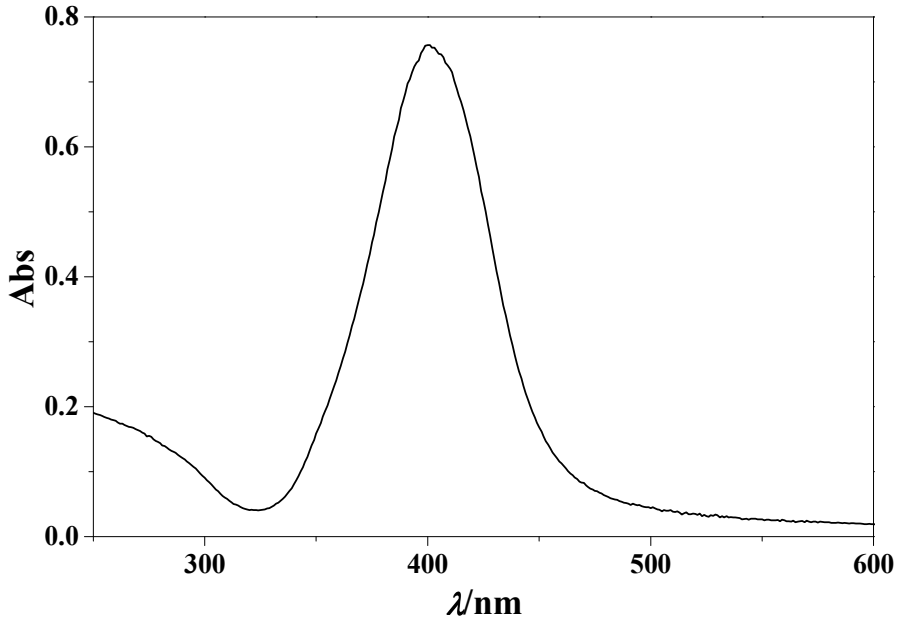

Fig. 2

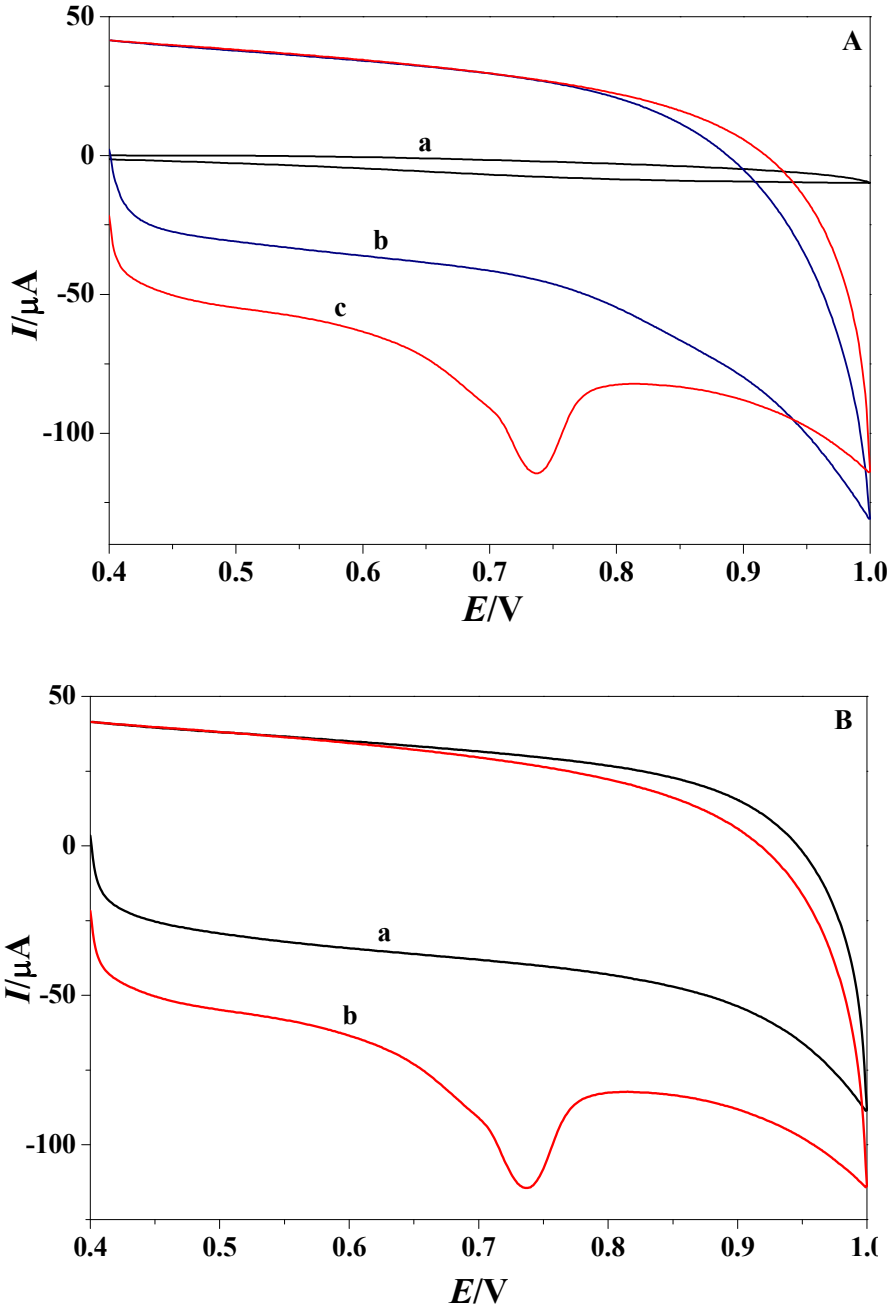

Fig. 3

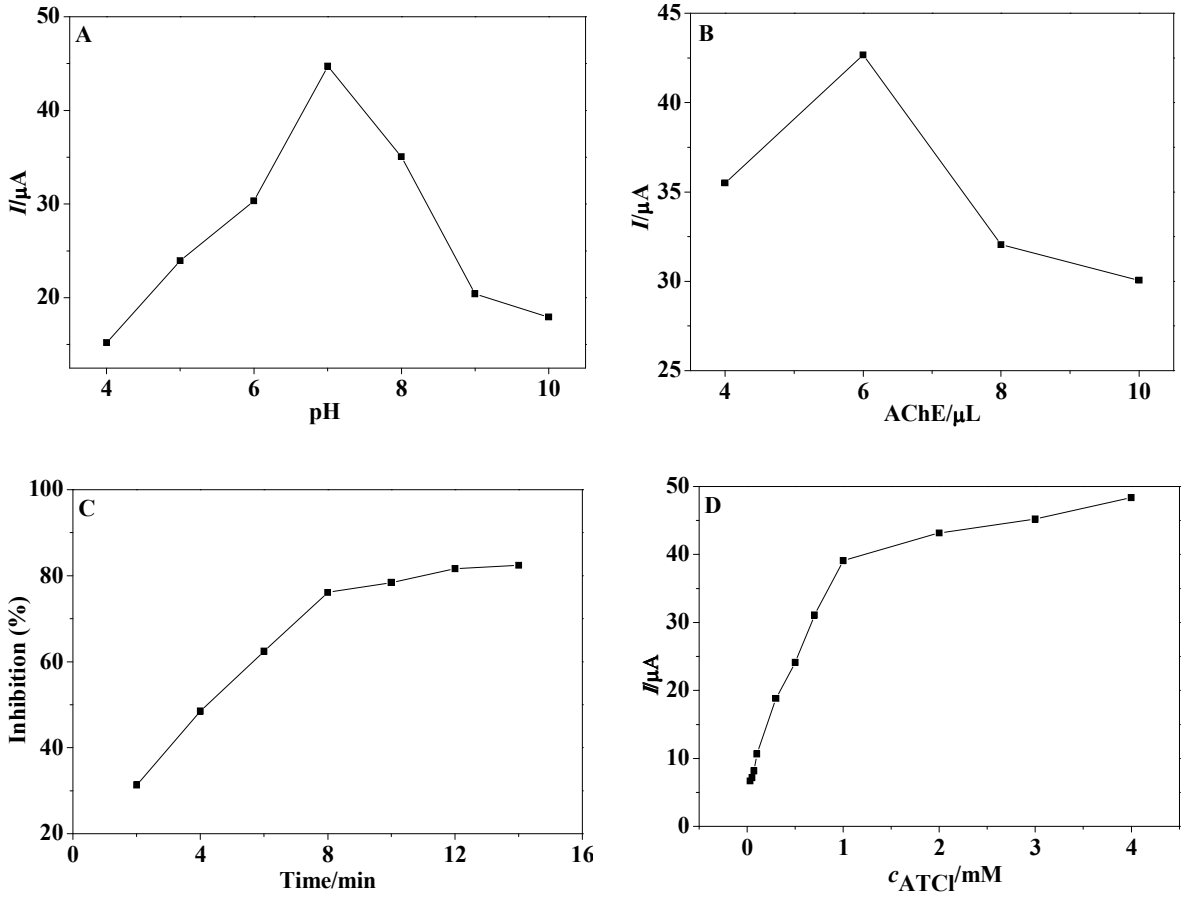

Fig. 4

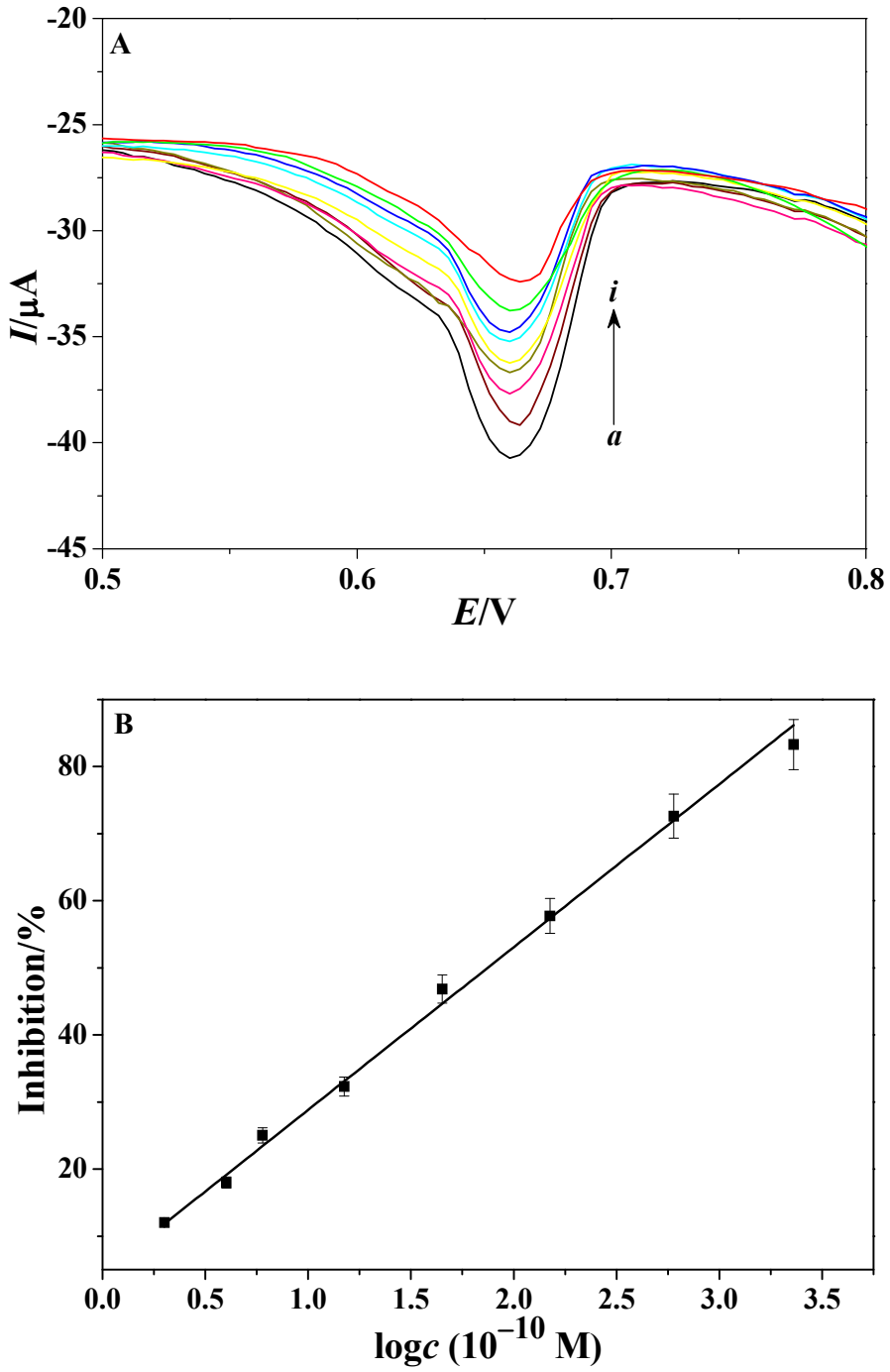

Fig. 5

Table 1

Comparison of performance of the other electrochemical sensors for phoxim detection[a]

Electrode	Technique	Linearity (nM)	Detection limit (nM)	References
Gold NEEs	*i* – *t*	59 – 12000 μM	4.8 μM	32
AChE/ZrO_2/Chit/GCE	*i* – *t*	6.6 – 440 μM	1.3 μM	33
AChE-AuNPs-SF/Pt	*i* – *t*	5 – 20	2	34
AChE/PB/GCE	*i* – *t*	0.17 – 33	0.033	35
GR/GCE	LSV	20 – 20000	8	36
Chit/AChE/$SnSe_2$/GCE	CV	26.8 – 17000	13.4	37
P3MT/NGE/GCE	CV	20 – 200	6.4	38
rGO/AuNPs/GCE	DPV	10 – 10000	3	39
AChE@CChit/AgNCs/rGO/GCE	DPV	0.2 − 250	0.081	This work

[a] NEEs: nanoelectrode ensembles; SF/Pt: silk fibroin/platinum electrode; PB: prussian blue; P3MT/NGE: poly(3-methylthiophene)/nitrogen doped graphene; *i* – *t*: chronoamperometry; LSV: linear sweep voltammetry.

Table 2 Determined results of phoxim in spiked water samples (n = 5)

Sample	Added (M)	Found (M)	Recover (%)	RSD (%)
1	0	Not detected	–	–
2	1×10^{-9}	0.91×10^{-9}	91.2	4.2
3	5×10^{-9}	4.83×10^{-9}	96.6	3.7
4	1×10^{-8}	0.90×10^{-8}	89.7	5.5